



Contents lists available at ScienceDirect

Defence Technology

journal homepage: [www.elsevier.com/locate/dt](http://www.elsevier.com/locate/dt)

# Magnetic, thermal stability and dynamic mechanical properties of beta isotactic polypropylene/natural rubber blends reinforced by NiZn ferrite nanoparticles

Lih-Jiun Yu <sup>a,\*</sup>, Sahrim Hj Ahmad <sup>b</sup>, Ing Kong <sup>c</sup>, Mouad A. Tarawneh <sup>d</sup>,  
Shamsul Bahri Bin Abd Razak <sup>e</sup>, Elango Natarajan <sup>a</sup>, Chun Kit Ang <sup>a</sup>

<sup>a</sup> Department of Mechanical Engineering, Faculty of Engineering, Technology and Built Environment, UCSI University, No 1, Jalan Menara Gading, UCSI Heights (Taman Connaught), Cheras, 56000, Kuala Lumpur, Malaysia

<sup>b</sup> School of Applied Physics, Faculty of Science and Technology, University Kebangsaan Malaysia, 43600, Bangi, Selangor Darul Ehsan, Malaysia

<sup>c</sup> School of Engineering and Mathematical Sciences, La Trobe University, Bundoora, VIC, 3086, Australia

<sup>d</sup> Department of Physics, College of Science, Al-Hussein Bin Talal University, P.O Box 20, Ma'an, Jordan

<sup>e</sup> Department of Food Science and Technology, University Malaysia Terengganu, Kuala Nerus, Terengganu, Malaysia

## ARTICLE INFO

### Article history:

Received 10 January 2019

Received in revised form

14 February 2019

Accepted 6 March 2019

Available online xxx

### Keywords:

Magnetic

Thermoplastic natural rubber

Nanoparticles

Composites

## ABSTRACT

The dispersion of magnetic nanoparticles in matrix is crucial to ensure optimum performance of the composite. The difficulty level of achieving good dispersion is further increase when a multi-phases of matrix is present. A pre-coating technique of magnetic nanoparticles with polypropylene using ball-mill prior to melt-blending process was employed to prepare a multi-phases thermoplastic natural rubber composite. The effect of filler loading (2 wt%-10 wt%) on morphology, structure, magnetic properties, thermal stability and dynamic mechanical properties of the composites were investigated. It was found that the NiZn ferrite nanoparticles act as nucleating agent to form beta isotactic polypropylene thermoplastic composites. The composites' magnetic properties are directly dependent on the filler concentration. The dispersion of magnetic fillers in polymer matrix plays role in affecting the magnetic properties and thermal stability. The preference of filler to locate at amorphous phase has distorted the chain orientation of natural rubber and polypropylene. Hence, the polymorphism and crystallinity of the matrix varied as the filler loading increased, affecting the dynamic mechanical properties. It was found that 8 wt% NiZn nanocomposite exhibits highest  $E'$  and  $\tan\delta$ , indicating the dynamic mechanical properties of NiZn nanocomposite are affected by  $\beta$ -phase degree.

© 2019 The Authors. Published by Elsevier Ltd. This is an open access article under the CC BY-NC-ND license (<http://creativecommons.org/licenses/by-nc-nd/4.0/>).

## 1. Introduction

Thermoplastic natural rubber (TPNR) is an analogue of the thermoplastic elastomers (TPE). They are prepared by blending rubber with thermoplastics such as polyolefins, offering an intermediate properties between these two polymers. According to Ibrahim & Dahlan [1], the TPNR exhibits improved impact strength, ductility and stiffness, as compared to the rubber and polyolefins. In

addition, the ease of processing and high recycling ability are the main advantages of the TPE. Various fillers were incorporated into the thermoplastic elastomer matrices, aimed to achieve desired properties in the specific application. However, there is a need for proper mixing between the fillers and TPNR matrix in order to achieve optimal results.

Incorporation of ferrite nanoparticles in polymeric matrix has offered superior performance in microwave absorption [2–6] and information storage [7–9], potentially applicable in stealth technology [10] and energy storage. The ferrite nanoparticles are embedded in polymeric matrix, enhancing the magnetic properties and mechanical properties of the polymers [1,11–13]. These composite materials offer advantages, in term of flexibility of shaping, cost saving and reducing environmental attack on the filler counterparts. However, a good dispersion of the magnetic fillers in

\* Corresponding author.

E-mail addresses: [yulj@ucsiuniversity.edu.my](mailto:yulj@ucsiuniversity.edu.my) (L.-J. Yu), [sahrim@ukm.my](mailto:sahrim@ukm.my) (S.H. Ahmad), [i.kong@latrobe.edu.au](mailto:i.kong@latrobe.edu.au) (I. Kong), [moath20042002@yahoo.com](mailto:moath20042002@yahoo.com) (M.A. Tarawneh), [shamsul@umt.edu.my](mailto:shamsul@umt.edu.my) (S.B.B. Abd Razak), [elango@ucsiuniversity.edu.my](mailto:elango@ucsiuniversity.edu.my) (E. Natarajan), [ckang@ucsiuniversity.edu.my](mailto:ckang@ucsiuniversity.edu.my) (C.K. Ang).

Peer review under responsibility of China Ordnance Society

polymer matrix is hard to achieve, magnetic particles have higher tendency to form agglomerate due to their magnetic interaction. Furthermore, the control of fillers dispersion could be tougher, especially when the fillers are incorporated into multiple phase matrix. Premphet & Horanont [14] observed that the phase structure of the ternary phase composite can be either exhibits as a separate dispersion of the phases or encapsulation of the fillers by elastomer. These two phase structure showed different crystallization behavior and dynamic mechanical properties, depends on the polarity of the elastomer.

Numerous studies emphasized on the preparation and characterization of  $\beta$  isotactic polypropylene [15–19]. The formation of  $\beta$  isotactic polypropylene with the presence of nucleating agent in multiple phase thermoplastic blends and their properties are remained unclear. In this paper, the work focused on the relationship between the microstructure and the properties of the NiZn ferrite loading in binary phase matrix which consists of natural rubber and polypropylene. The effect of filler loading on magnetic properties, thermal stability and dynamic mechanical properties of the nanocomposites were studied.

## 2. Materials and methods

Nickel zinc ferrite nanoparticles ( $\text{Ni}_{0.5}\text{Zn}_{0.5}\text{Fe}_2\text{O}_4$ ), with 98.5% purity, average particle size 10–30 nm, were obtained from commercial suppliers in powder form. Natural Rubber (NR) and polypropylene (PP) were supplied by the Rubber Research Institute of Malaysia (RRIM) and Mobile (M) Sdn. Bhd. Liquid natural rubber (LNR) was prepared by photosynthesized degradation of NR in visible light.

The TPNR was prepared from PP, NR and LNR with a weight ratio of 70:20:10. LNR was used as the compatibilizer in the mixture.  $\text{NiZnFe}_2\text{O}_4$  nanopowder was ball milled with PP for 15min prior incorporated in the TPNR matrix by melt blending techniques in the laboratory. In this study, the TPNR/ $\text{NiZnFe}_2\text{O}_4$  nanocomposite with 2 wt%–10 wt%  $\text{NiZnFe}_2\text{O}_4$  was prepared using Thermo Haake at rotation speed of  $100\text{r} \cdot \text{min}^{-1}$ ,  $180^\circ\text{C}$ , for 13min. After the blend, the samples were hot-pressed into a thin sheet of 1 mm in thickness using a hydraulic press at  $185^\circ\text{C}$ . Field emission scanning electron microscopy (FESEM) graph for the nanocomposite was obtained from a fractured surface. Transmission electron microscopy (TEM) graph for the nanocomposite was obtained by Phillips CM-12. Microstructure studies on nanocomposites were carried out by X-ray diffraction (XRD; Siemens D5000) with  $\text{CuK}\alpha_1$  radiation ( $\lambda = 1.5406 \text{ \AA}$ ). Magnetization measurements were carried out using a vibrating sample magnetometer, VSM (Model 7404), to obtain the M – H loop at room temperature ( $25^\circ\text{C}$ ). Thermogravimetric analysis and dynamic mechanical analysis were carried out using TGA 50 (Shimadzu) and DMA 2980 (TA instrument) respectively.

## 3. Results

### 3.1. Magnetic properties

The hysteresis of pure NiZn nanoparticles and nanocomposites with different filler content was measured at room temperature. Fig. 1 exhibits the loops for the six samples with 2 wt%, 4 wt%, 6 wt%, 8 wt%, 10 wt% and 100 wt% of NiZn ferrite. The corresponding results from VSM for all samples are listed in Table 1. Initial susceptibility and permeability of the nanocomposite were obtained from the initial magnetization curve from VSM and listed in Table 1. As the filler content increased, the values of saturation magnetization ( $M_s$ ), remanence ( $M_R$ ), initial susceptibility ( $\chi_i$ ), and initial permeability ( $\mu_i$ ) increased, except for coercivity ( $H_{ci}$ ). The results are consistent with previous reports on other magnetic polymer by

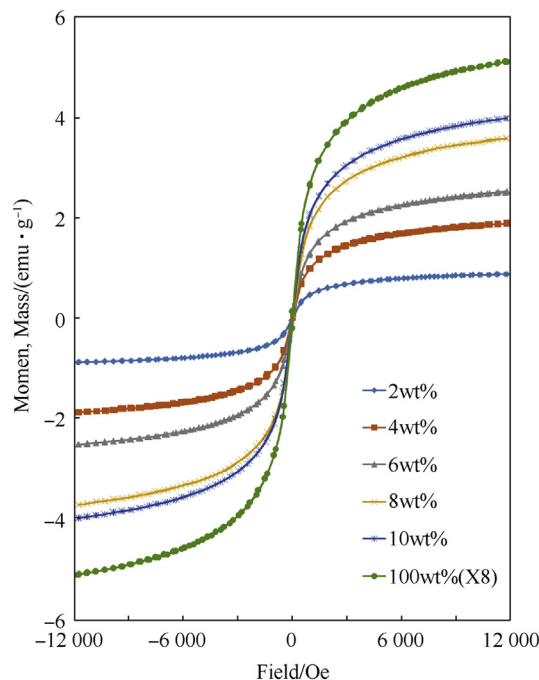


Fig. 1. M – H hysteresis loop obtained from the samples with various filler loading.

Table 1

Corresponding results obtained from VSM.

wt%	$M_s$ /emu · g <sup>-1</sup>	$H_{ci}$ /Oe	$M_R$ /emu · g <sup>-1</sup>	$\chi_i$ /(emu · cm <sup>-3</sup> )Oe	$\mu_i$ —
2	0.791	22.06	0.014	0.009	1.012
4	1.875	21.65	0.032	0.017	1.021
6	2.299	21.12	0.038	0.021	1.027
8	3.614	20.76	0.058	0.032	1.040
10	4.073	20.69	0.065	0.041	1.051
100	41.18	20.35	0.614	0.165	3.076

Kong et al. [2] and Gokturk et al. [20]. For all nanocomposites, it is observed that the initial permeability is lower than 100 wt% NiZn ferrite. This is because the ferrite grains are embedded in the TPNR matrix. Vijutha Sunny [13] suggests that the nonmagnetic rubber matrix causes a discontinuity in the nanocomposite giving way to a demagnetizing field, thus, reducing the permeability at lower filler contents.

The results indicate that saturation magnetization and remanence are increasing whereas the intrinsic coercive force value show a slightly decreasing, ranging from 22.06 to 20.35Oe. The  $H_{ci}$  values of the nanocomposite are close to the  $H_{ci}$  value of 100 wt% of NiZn ferrite (20.35Oe). The values are different from those previously reported by Ramajo et al. [21] and Yang et al. [22], as the  $H_{ci}$  values of magnetic composites are almost constant and independent to the filler loading. It is known that the coercive force of a material is sensitive to the microstructure, related to the anisotropy of the magnetic particle. A good mixing process enables the magnetic particles to be randomly orientated and dispersed uniformly in the polymer matrix. The magnetic particles are isolated from each other in the polymer matrix. This could reduce the agglomeration of the magnetic particles, giving a higher mean distance between the particles. As the mean interparticle distance increases, the magnetic interaction between the ferrite particles decreases. The TPNR matrix restricts the alignment of the magnetic moment of the ferrite. Therefore, it is hard to demagnetize the ferrite

particles with higher mean distance between the particles, thus the coercive force is high in the lower ferrite loading in the composite. Fig. 2 shows SEM micrograph of the fractural surface of 2 wt% and 10 wt% of NiZn ferrite nanocomposite. The white spheres embedded in the TPNR matrix are NiZn ferrite nanoparticles. The NiZn ferrite particles in 10 wt% nanocomposites have a higher tendency to agglomerate into larger size, leaving a large interparticle distance between the nanoparticles while NiZn ferrite particles in 2 wt% nanocomposites are closed and isolated by the matrix.

Application of a field  $H$  causes the magnetic induction to increase in the field direction. Magnetization reaches saturation when all the magnetic dipoles within the materials are aligned in the direction of the magnetic field. The saturation magnetization is only dependent only on the magnitude of the atomic magnetic moments  $m$  and the number of atoms per unit volume  $n$ ,  $M_s = nm$ . Saturation magnetization is also commonly expressed as the magnetic moment per mass. This specific saturation magnetization is linearly dependent on the mass fraction of ferrite and obeys the general relation:  $M_s = M_f W_f$ . Where  $M_f$  and  $W_f$  are the saturation magnetization and weight fraction of the ferrite, respectively. The saturation magnetization of the nanocomposite depends on the content of the filler with magnetic moments in a given mass fraction. The experimental  $M_s$  value and the theoretical  $M_s$  value were plotted in Fig. 3. The results indicate good agreement, as both experimental and theoretical  $M_s$  values are similar.

### 3.2. Crystallography structure

The X-ray diffractograms of the TPNR and nanocomposites with various filler loadings are shown in Fig. 4. The figure illustrates that two phases, crystalline phase and amorphous phase co-exist in both the TPNR and the nanocomposites. For all samples, the semi-amorphous phases of the TPNR appear at the lower  $2\theta$  degree ( $<30^\circ$ ) and  $42.48^\circ$ . According to Alariqi et al. [23], the sharp peaks ( $14.05^\circ$ ,  $16.9^\circ$ ,  $18.5^\circ$ ,  $21.8^\circ$ ) in this range contributed by the

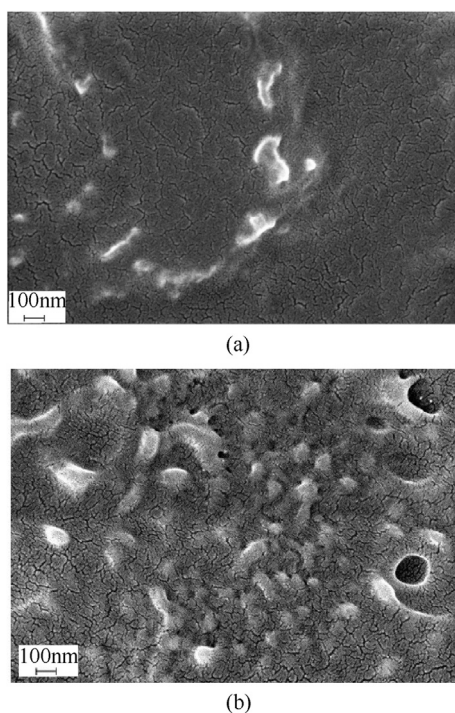


Fig. 2. FESEM micrograph of (a) 2 wt% NiZn ferrite nanocomposite (b) 10 wt% NiZn ferrite nanocomposite.

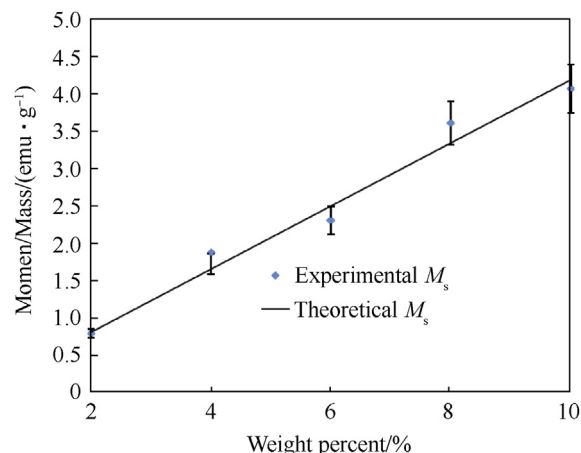


Fig. 3. Comparison of theoretical and experimental  $M_s$  values.

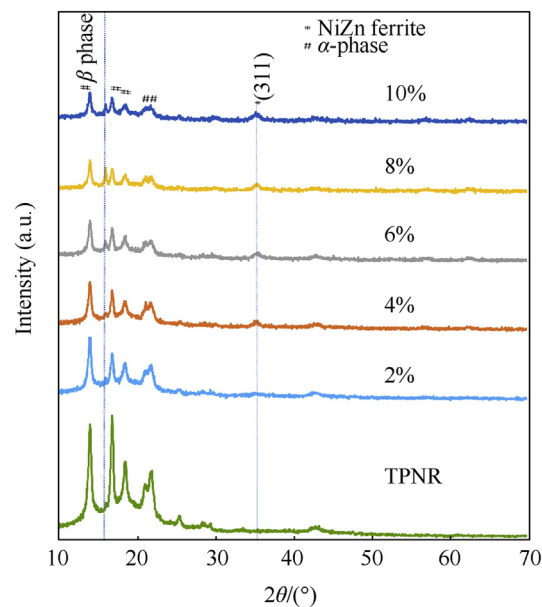


Fig. 4. X-ray diffractograms of the nanocomposites with different filler content.

crystallinity of the  $\alpha$ -phase isotactic PP. Meanwhile, the broadening of the amorphous region of NR could be seen clearly in the X-ray diffractogram of TPNR. Tang et al. [24], Wang et al. [25] and Jancar [26] agreed that the thermodynamically stable  $\beta$ -phase formation of polymorphic PP is hard to achieve under normal processing condition. Varga et al. [27] and Horvath et al. [28] stated that the  $\beta$ -phase can be obtained when the PP undergoes isothermal crystallization process, high shear field crystallization process or blended with  $\beta$ -phase nucleating ability polymer. It can be seen that the  $\beta$ -phase PP which located at  $16^\circ$  appears when NiZn ferrite incorporated in the TPNR. The proportional increment of the intensities  $\beta$ -phase with the filler content under constant processing condition, has demonstrated that the ability of NiZn ferrite to act as a nucleating agent, to promote  $\beta$ -phase formation of PP. The highest relative content of  $\beta$ -phase PP were obtained at 8 wt% NiZn ferrite, then reduced 25% at 10 wt% NiZn ferrite. The tendency of NiZn ferrite particle to form agglomerates at high filler content has weakened the nanoscale confinement structure formation, resulted disoriented PP crystals formation, hence led to an overall reduction in crystallinity of PP. The characteristic peaks of NiZn ferrite



matched with the database (JCPDS file no. 00-008-0234) to confirm the planes of NiZn ferrite in the nanocomposites. There is no structural change NiZn ferrite after incorporating in the TPNR, because the peak position of the NiZn ferrite peaks remain unchanged. It can be seen that, the increment of NiZn ferrite loading leads to the increment of the intensity of the characteristic peaks for NiZn ferrite, significantly at the major intensity peak at plane (311). By referring to the NiZn ferrite peaks in plane (311), the fractional crystallinity of the nanocomposites are 0.51, 0.52, 0.54, 0.62, 0.87 for 2 wt%-10 wt% nanocomposites respectively. Diffraction peaks and the amorphous phase of TPNR reduced at higher filler content since the characteristic peaks of crystalline NiZn ferrite became dominant. This result is consistent with Sun et al. [11] and Low et al. [29]. The crystallinity and amorphous region of TPNR were suppressed after introducing fine NiZn ferrite particles into the system, due to the migration of fine particles interfering the preferred orientation of the TPNR. The magnetic dipole interaction of NiZn ferrite is higher in the low crystalline matrix because of the higher freedom of spin rotation at the amorphous phase, hence, leading to better magnetization properties NiZn ferrite in TPNR. At higher filler loadings, more NiZn ferrite particles located in the amorphous phase. Therefore, less external force ( $H_{ci}$ ) is required to orientate spin according to the applied field.

Fig. 5 illustrates the TEM micrograph of the NiZn ferrite nanocomposite. The dark spheres are NiZn ferrite particles, the grey regions are the NR phase, and the white regions are the PP phase. The phase structure of the NiZn ferrite nanocomposites shown in Fig. 5 is the combination of the two types of phase structure, which observed by Premphet & Horanont [14]. It can be seen that the NiZn ferrite particles are distributed homogenously in both the NR and PP phase, while some aggregation of the NiZn ferrite particles is likely to occur in the NR phase, due to the slightly high viscosity of NR, which limits the dispersion of NiZn ferrite particles during the mixing process. According to Osawa et al. [30], the movement of polymer segment surrounded the filler was limited by polymer-particle interaction. Hence, the preference of NiZn ferrite particles to aggregate in NR phases leads to the rapid drop of crystallinity of the TPNR phase. Based on the morphology examination, a schematic diagram was drawn to show the phase structure of the NiZn ferrite nanocomposite. Fig. 6 (a) shows the arrangement of TPNR molecule chains which consist of semi-crystalline phase and amorphous phase. After incorporated with NiZn ferrite with higher electronegative attraction, the molecule chain of TPNR was distorted by the NiZn ferrite particles with higher electronegative attraction and hence, affected the TPNR crystallography structural, as shown in Fig. 6 (b).

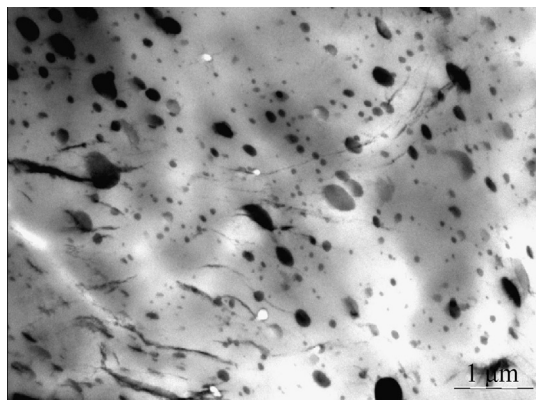


Fig. 5. TEM micrograph of 2 wt% NiZn ferrite nanocomposite.

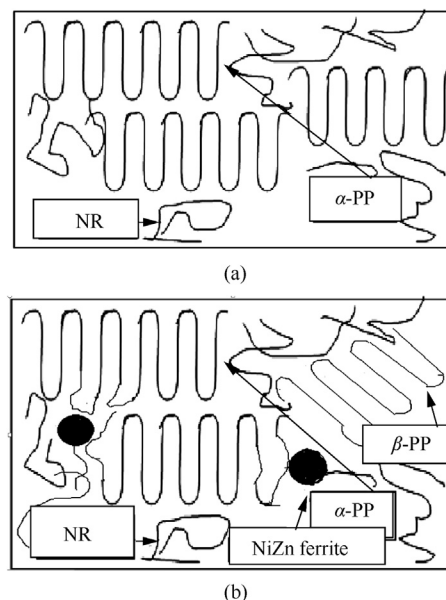


Fig. 6. Schematic diagram of the arrangement of the TPNR molecule chains (a) before incorporated with NiZn ferrite (b) after incorporated with NiZn ferrite.

### 3.3. Thermal properties

The thermal stability of the NiZn ferrite nanocomposite was studied by thermogravimetry analysis under the nitrogen flow to prevent unwanted weight addition of oxidized product during heating process and was illustrated in Fig. 7. The corresponding data obtained from thermogram are listed in Table 2. It was found that the thermal degradation of TPNR and its nanocomposites takes place through a two-step process, remarkable at decomposition temperature around 360 °C and 440 °C. The first decomposition

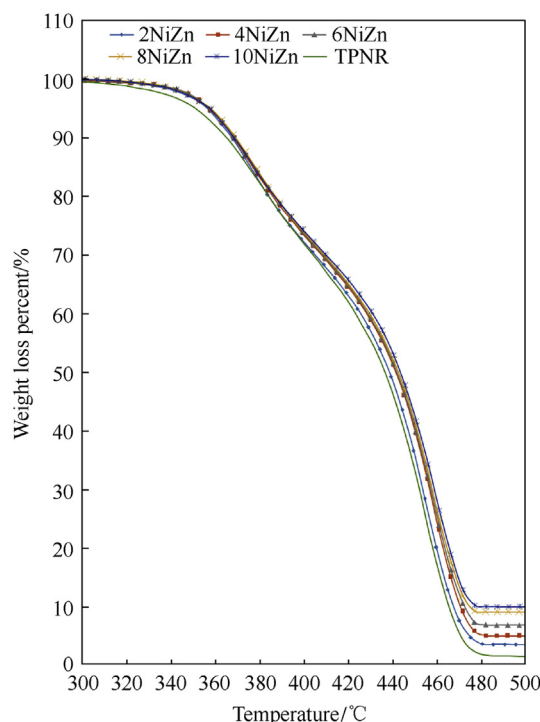


Fig. 7. Thermogram of NiZn ferrite nanocomposite.

**Table 2**

Data obtained from thermogram graph.

Nanocomposite	$T_{10}/^{\circ}\text{C}$	$T_{50}/^{\circ}\text{C}$	$T_T/^{\circ}\text{C}$	Residual Weight/%
TPNR	366.0	437.0	484.5	0.47
2 wt% NiZn	367.0	438.0	479.5	1.93
4 wt% NiZn	368.5	441.0	478.0	3.61
6 wt% NiZn	369.5	442.0	477.5	5.73
8 wt% NiZn	370.5	442.5	477.0	7.52
10 wt% NiZn	370.0	443.5	467.5	8.93

temperature was due to the decomposition of the NR phases while the latter was due to the decomposition of the PP phases. The difference of crystallinity degree of these two phases impacts to the decomposition temperature, whereas the lower crystallinity phase (NR) provided more free volume to enable the molecules movement during heating process. The NiZn ferrite has higher resistance to the thermal degradation because the molecules are highly crystalline oriented. The thermal decomposition temperature of NR phases and PP phases of the NiZn ferrite nanocomposites were studied at the 10% weight loss and 50% weight loss of samples, denoted by  $T_{10}$  and  $T_{50}$  respectively in Table 2. The results revealed that the  $T_{10}$  and  $T_{50}$  are slightly shifted to the higher value. It is clear that the addition of NiZn ferrite leads to an increase of the TPNR thermal stability. Similar thermal stability behavior of the addition ferrite has been reported by Cha & Kim (2007) [31] and Puryanti et al. (2007) [32]. The delaying of volatile products diffuse from bulk polymer was attributed to the physical absorption between the NiZn ferrite surface and their surrounding TPNR molecule chains. The increment of NiZn ferrite content provided more absorption interaction with the TPNR molecules, hence retarded the decomposition process of both NR phases and PP phases. The endset temperature of the nanocomposite was denoted by  $T_T$ . Apparently, the values of  $T_T$  are inversely proportionally to the NiZn ferrite content, due to more heat energy are required to decompose large quantity of hydrocarbon compounds that presence in the samples. The residual weight percent demonstrated the remaining carbonyl products and NiZn ferrite which are incombustible at 500 °C. These residual weight percent approached the initial filler weight percent, indicating a homogeneity blends were achieved by the blending of NiZn ferrite into the TPNR matrix.

### 3.4. Dynamic mechanical properties

The temperature dependence of storage modulus ( $E'$ ) of different filler loading of NiZn ferrite nanocomposite were studied at the fixed frequency of 1 Hz. From Fig. 8 (a), the NiZn ferrite addition had induced a higher  $E'$  value at  $-80^{\circ}\text{C}$ . The large particle surface of nanosized NiZn ferrite tends to increase the stiffness of the TPNR in glassy state. Diez-Pascual et al. [33] explained the increment of  $E'$  value is attributed to the effective load transfer from the polymer matrices to the fillers, resulting from the good dispersion of fillers in the matrix. The  $E'$  value of 2 wt% NiZn ferrite showed a drastic drop at  $-73^{\circ}\text{C}$  and exhibited lowest  $E'$  values above its glass transition temperature; this result is in agreement with Varga et al. [27] findings, the formation of  $\beta$ -phase PP reduced the tensile strength of nanocomposite, provided higher impact strength and ductility in contrast. However, as NiZn ferrite loading increases, the  $\beta$ -phase's toughening effect was overtaken by the reinforcement effect of the NiZn ferrite nanoparticle. Highest  $E'$  was achieved by 8 wt% NiZn ferrite, further increment of NiZn ferrite loading was found ineffective in load transfer. The reduction of  $E'$  at 10 wt% possible due to reduction in  $\beta$ -phase PP and agglomeration of NiZn ferrite nanoparticles.

From Fig. 8 (b),  $\tan\delta$  peak value of all nanocomposites is higher

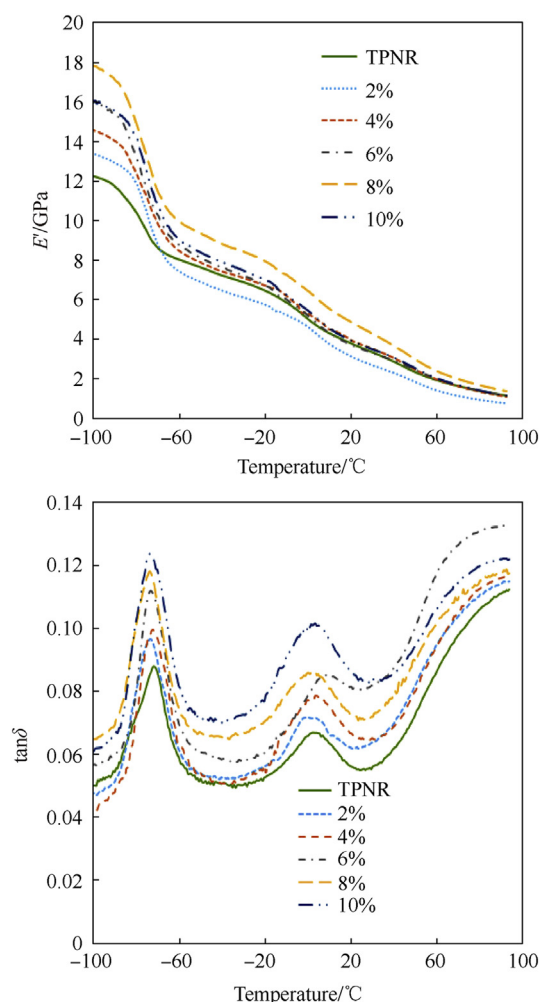


**Fig. 8.** (a) Storage modulus of nanocomposites with various filler loading (b)  $\tan\delta$  of nanocomposite with various filler loading.

than the corresponding  $\tan\delta$  peak value of TPNR. The increasing trend of the  $\tan\delta$  peak values was contributed by the hysteresis loss upon dynamic tensile stress. This is probably due to the particle-particle friction and particle-matrix interface interaction when more filler were introduced to the TPNR matrix. The particle-matrix interface interaction due to the presence of  $\beta$ -phase around the NiZn ferrite particle resulted increasing in the damping characteristic of the nanocomposites. Similar increment of  $\tan\delta$  peak value was observed by Weon & Sue [34] in the  $\text{CaCO}_3$ /high crystalline PP system with the presence of  $\beta$ -phase. The corresponding glass transition temperatures ( $T_g$ ) of the TPNR and the NiZn nanocomposites were identified from the  $\tan\delta$  peak position. It can be seen that there are two glass transition temperatures as shown by TPNR and NiZn nanocomposites. The first  $T_g$  (approximately  $-70^{\circ}\text{C}$ ) is the  $T_g$  for NR, while the latter glass transition temperature approximately located at  $11^{\circ}\text{C}$  is the  $T_g$  for PP in the TPNR system. The results shows the both  $T_g$  values had shifted to the lower value after incorporated with the NiZn ferrite particles. This implies that the incorporation of fillers in the TPNR matrix induced  $\beta$ -phase formation, led to an increment in the free volume of the polymer chain, thus promotes the molecular mobility at lower temperature. It can be observed that both glass transition temperatures (NR and PP) of 8 wt% NiZn nanocomposite is relatively low (approximately  $-73^{\circ}\text{C}$  and  $4^{\circ}\text{C}$ ). This is corresponding to high degree of  $\beta$ -phase presents in 8 wt% NiZn

nanocomposite, resulting in more molecular chains mobility. The loss of energy attributed to the lower cohesive force by the  $\beta$ -phase, leads to easier slipping on the lamella chains when the degree of  $\beta$ -phase increased [35].

#### 4. Conclusions

Thermoplastic natural rubber exhibits as a non-magnetic material. The magnetic properties of TPNR can be improved by incorporating magnetic particles. It was found that the magnetic properties of the nanocomposites improved as the ferrite loading increased. The saturation magnetization of the nanocomposites can be estimated by its weight fraction of filler loading, following linear proportion of filler magnetization and its weight fraction relationship. The reduction of crystallinity of TPNR leads to higher magnetization properties due to the higher degree of spin rotation of the NiZn ferrite particles available in the amorphous phases. NiZn ferrite was found to act as a  $\beta$ -phase nucleating agent in the ternary phase composite, with the aids of pre-coating technique. The thermal stability, stiffness and softening point of the thermoplastic natural rubber were enhanced with the NiZn ferrite addition. It was found that 8 wt% NiZn nanocomposite exhibits highest  $E'$  and  $\tan\delta$ , indicating that the dynamic mechanical properties of NiZn nanocomposite are improved with increment of  $\beta$ -phase degree.

The scope of this work was limited to a fixed ternary phase blend ratio of PP: NR: LNR. The work could be extended to investigate effect of beta isotactic polypropylene formation when different ratio of ternary blend is applied.

#### Conflicts of interest

The authors declare no conflict of interest.

#### Acknowledgments

The authors would like to thank the support from the National Science Fund (NSF), MOSTI, UKM and UCSI.

#### References

- [1] Ibrahim A, Dahlan M. Thermoplastic natural rubber blends. *Prog Polym Sci* 1998;23:665–706.
- [2] Ghodake JS, Kambale RC, Shinde TJ, Maskar PK, Suryavanshi SS. Magnetic and microwave absorbing properties of  $\text{Co}^{2+}$  substituted nickel-zinc ferrites with the emphasis on initial permeability studies. *J Magn Magn Mater* 2016;401:938–42.
- [3] Huang X, Zhuang J, Lai M, Sang TX. Preparation and microwave absorption mechanisms of the NiZn ferrite nanofibers. *J Alloy Comp* 2015;627:367–73.
- [4] Ren X, Xu GX. Electromagnetic and microwave absorbing properties of NiCoZn-ferrites doped with  $\text{La}^{3+}$ . *J Magn Magn Mater* 2014;354:44–8.
- [5] Yu LJ, Sahrim HA, Sivanesan A, Kong I. Comparison of magnetic and microwave absorbing properties between multiwalled carbon nanotubes nanocomposite, nickel zinc ferrite nanocomposite and hybrid nanocomposite. *World J Eng* 2014;11:317–22.
- [6] Ali NN, Atassi Y, Salloum A, Charba A, Malki A, Jafarian M. Comparative study of microwave absorption characteristics of (polyaniline/NiZn ferrite) nanocomposites with different ferrite percentages. *Mater Chem Phys* 2018;211:79–87.
- [7] Sharma R, Thankur P, Sharma P, Sharma V. Ferrimagnetic  $\text{Ni}^{2+}$  doped Mg-Zn spinel ferrite nanoparticles for high density information storage. *J Alloy Comp* 2017;704:7–17.
- [8] Fu M, Chen W, Zhu X, Liu Q. One-step preparation of one dimensional nickel ferrites/graphene composites for supercapacitor electrode with excellent cycling stability. *J Power Sources* 2018;396:41–8.
- [9] Wang D, Wu J, Wang R, Yao F, Xu S. Mesoporous spinel ferrite composite derived from a ternary  $\text{MgZnFe}$ -layered double hydroxide precursor for lithium storage. *J Alloy Comp* 2017;726:306–14.
- [10] Kolanowska A, Janas D, Herman AP, Jedrysiak RG, Gizewski T, Boncel S. From blackness to invisibility—Carbon nanotubes role in the attenuation of and shielding from radio waves for stealth technology. *Carbon* 2018;126:31–52.
- [11] Kong I, Ahmad SH, Abdullah MH, David H, Yusoff AN, Puryanti D. Magnetic and microwave absorbing properties of magnetite-thermoplastic natural rubber nanocomposites. *J Magn Magn Mater* 2010;322:3401–9.
- [12] Makled MH, Matsui T, Tsuda H, Mabuchi H, El-Mansy MK, Morii K. Magnetic and dynamic mechanical properties of barium ferrite-natural rubber composites. *J Mater Process Technol* 2005;160:229–33.
- [13] Sunny V, Philip Kurian P, Mohanan P, Joy PA, Anantharam MR. A flexible microwave absorber based on nickel ferrite nanocomposite. *J Alloy Comp* 2010;489:297–303.
- [14] Premphet K, Horanont P. Phase structure of ternary polypropylene/elastomer/filler composites: effect of elastomer polarity. *Polymer* 2000;41:9283–90.
- [15] Menyhard A, Gahleitner M, Varga J, Bernreiter K, Jaaskelainen P, Oysaed H, Pukanszky B. The influence of nucleus density on optical properties in nucleated isotactic polypropylene. *Eur Polym J* 2009;45:3138–48.
- [16] Roozmond PC, Erp TBV, Peters GWM. Flow-induced crystallization of isotactic polypropylene: modeling formation of multiple crystal phases and morphologies. *Polymer* 2016;89:69–80.
- [17] Housmans J-W, Gahleitner M, Peters GWM, Meijer HEH. Structure-property relations in molded, nucleated isotactic polypropylene. *Polymer* 2009;50:2304–19.
- [18] Zhang X, Zhang D, Liu T. Influence of nucleating agent on properties of isotactic polypropylene. *Energy Procedia* 2012;17:1829–42.
- [19] Mollova A, Androsch R, Mileva D, Gahleitner M, Funari SS. Crystallization of isotactic polypropylene containing beta-phase nucleating agent at rapid cooling. *Eur Polym J* 2013;49:1057–65.
- [20] Gokturk HS, Fiske TJ, Kalyon DM. Electric and magnetic properties of a thermoplastic elastomer incorporated with ferromagnetic powders. *IEEE Trans Magn* 1993;29:4170–6.
- [21] Ramajo LA, Cristobal AA, Botta PM, Porto Lopez JM, Reboredo MM, Castro MS. Dielectric and magnetic response of  $\text{Fe}_3\text{O}_4$ /epoxy composites. *Compos Part A* 2009;40:388–93.
- [22] Yang HB, Wang H, Xiang F, Yao X. Multifunctional  $\text{SrTiO}_3/\text{nizn}$  ferrite/POE composites with electromagnetic and flexible properties for RF application. *J Electroceram* 2009;22:221–6.
- [23] Alarqi SAS, Pratheep Kumar A, Rao BSM, Singh RP. Effect of  $\gamma$ -dose rate on crystallinity and morphological changes of  $\gamma$  sterilized biomedical polypropylene. *Polym Degrad Stabil* 2009;94:272–7.
- [24] Tang XG, Yang W, Bao RY, Shan GF, Xie BH, Yang MB, Hou M. Effect of spatial confinement on the development of  $\beta$  of polypropylene. *Polymer* 2009;50:4122–7.
- [25] Wang SW, Yang W, Bao RY, Wang B, Xie BH, Yang MB. The enhanced nucleating ability of carbon nanotube-supported  $\beta$ -nucleating agent in isotactic polypropylene. *Colloid Polym Sci* 2010;288:681–8.
- [26] Jancar J. Mineral fillers in thermoplastics I. Raw materials and processing. Berlin: Springer-Verlag Berlin Heidelberg; 1999. p. 54–65.
- [27] Varga J, Ehrenstein GW, Schlarb AK. *Express Polym Lett* 2008;2:148–56.
- [28] Zs Horvath, Sajo IE, Stoll K, Menyhard A, Varga J. The effect of molecular mass on the polymorphism and crystalline structure of isotactic polypropylene. *Express Polym Lett* 2010;4:101–14.
- [29] Low SP, Ahmad A, Hamzah A, Rahman MYA. Nanocomposite solid polymeric electrolyte of 49% poly(methyl methacrylate)-grafted natural rubber-titanium dioxide-lithium tetrafluoroborate ( $\text{MG49-TiO}_2\text{-LiBF}_4$ ). *J Solid State Electrochem* 2010;11:2611–8. <https://doi.org/10.1007/s10008-010-1252-0>.
- [30] Osawa Z, Kawauchi K, Iwata M, Harada H. Effect of polymer matrices on magnetic properties of plastic magnets. *J Mater Sci* 1988;23:2637–44.
- [31] Cha DW, Kim BC, Byoung C. Thermal and rheological properties of highly concentrated PET composites with ferrite nanoparticles. *Compos Sci Technol* 2007;67:1348–52.
- [32] Puryanti D, Ahmad SH, Abdullah MH, Yusoff ANH. Effect of Nickel-Cobalt-Zinc ferrite filler on magnetic and thermal properties of thermoplastic natural rubber composites. *Int J Polym Mater* 2007;56:327–38.
- [33] Diez-Pascual AM, Naffakh M, Gomez MA, Marco C, Ellis G, Martinez MT, Anson A, Gonzalez-Dominguez JM, Martinez-Rubi Y, Simard B. Development and characterization of PEEK/carbon nanotube composites. *Carbon* 2009;47:3079–90.
- [34] Weon JI, Sue HJ. Mechanical properties of talc-and  $\text{CaCO}_3$ -reinforced high-crystallinity polypropylene composites. *J Mater Sci* 2006;41:2291–300.
- [35] Nitta K-H, Takashima T. Tensile properties in  $\beta$ -modified isotactic polypropylene. *Polypropylene IntechOpen* 2018:[1]–[19].